LOCAL, REGIONAL AND GLOBAL POINT DETERMINATION USING THREE-LINE IMAGERY AND ORBITAL CONSTRAINTS

Timm Ohlhof
Chair for Photogrammetry and Remote Sensing
Technical University Munich, Germany
Phone: +49-89-2105 2671, Fax: +49-89-280 95 73
E-Mail: timm@photo.verm.tu-muenchen.de

Commision III, Working Group 1

KEY WORDS: Orientation, Simulation, CCD, Extraterrestrial, Three-Line, Bundle Block Adjustment, Orbital Constraints, MOMS-02

ABSTRACT

The emphasis of that paper is point determination using spaceborne 3-line imagery and orbital constraints. In order to properly utilize the image information contained in conjugate point coordinates and the orbit information contained in tracking data, both data types have to be evaluated in a combined adjustment process. To this end, the conventional bundle block adjustment algorithm is supplemented by a rigorous dynamical modeling of the satellite motion to take orbital constraints into account.

For the forthcoming Mars96 HRSC/WAOSS experiment computer simulations on point determination have been performed to obtain a survey of the attainable accuracy at local, regional and global levels. Since WAOSS will image the entire planet, a closed block covering the entire Martian surface may be processed under ideal circumstances. Because of the extraordinary strength of the closed block and based on the complete image, orbit, attitude and ground control information, 60 m accuracy in X, Y and Z can be achieved. Moreover, the Mars rotation parameters can be improved up to factor 4.

The new approach was also tested with practical data. Image data of the multi-line camera MOMS-02 and TDRSS tracking data, both acquired during the German D2 mission, were evaluated together. An empirical accuracy of 10 m (0.7 pixel) in X, Y and Z was obtained with only 4 groups of ground control points. Thus the efficiency of the rigorous bundle adjustment approach integrating orbital constraints has been proved with practical data. For that reason, it will be routinely used for the MOMS-2P/PRIRODA mission to be launched in spring 1996.

1 INTRODUCTION

The most advanced camera concept for primary data acquisition makes use of 3 linear CCD sensor arrays. They offer the advantage that stereo images are acquired quasi simultaneously. The 3 CCD-lines are imaging different terrain at the same time, whereas the 3 lines image the same terrain at different times, as the sensor platform moves.

In the last few years the 3-line camera concept has been realized for experimental airborne as well as spaceborne projects and is now getting into a pre-operational stage. The main important camera systems based on the 3-line camera concept are:

- Monocular Electro-Optical Stereo Scanner (MEOSS) (Lanzl 1986)

- Modular Optoelectronic Multispectral Scanner (MOMS-02) (Seige, Meissner 1993)

- Digital Photogrammetric Assembly (DPA) (Müller et al. 1994)

- High Resolution Stereo Camera (HRSC) (Neukum et al. 1995)

- Wide-Angle Optoelectronic Stereo Scanner (WAOSS) (Sandau, Bärwald 1994)

- Wide Angle Airborne Camera (WAAC) (Eckardt 1995)

- Triplet Linear Scanner (TLS) (Murai et al. 1995)

MEOSS, DPA, WAAC and TLS are airborne projects, whereas MOMS-02, HRSC and WAOSS are designed for spaceborne applications. A common major objective of all projects is the realization of and the software development for a completely digital photogrammetric processing chain for 3-line imagery from primary data acquisition to the generation of Digital Terrain Models (DTM) and orthoimage maps.

In the following a brief description of the concept of point determination using orbital constraints is given, which is recommended for spaceborne applications. Computer simulations on point determination have been performed to obtain a survey of the attainable accuracy at local, regional and global levels. Furthermore, results of tests with practical spaceborne MOMS-02 imagery are presented. Finally, conclusions are drawn and an outlook is given.

2 POINT DETERMINATION USING ORBITAL CONSTRAINTS

2.1 Background

So far orbital constraints in satellite photogrammetry have been formulated as early as 1960 by Brown (cf. Case 1961, Light 1980) for the construction of a lunar control network from metric camera photographs during the Apollo mis-

597

International Archives of Photogrammetry and Remote Sensing. Vol. XXXI, Part B3. Vienna 1996

sions (Davis, Riding 1970). For Earth-orbiting satellites the use of short-arc orbital constraints has been studied by Lehner and Drescher (1987), Masaharu (1989), and Westin (1990) for the restitution of MEOSS and SPOT imagery.

The present work is suited to incorporate both short-arc and long-arc orbital constraints into the bundle block adjustment in a rigorous manner and has been developed especially for the photogrammetric restitution of 3-line imagery. Furthermore, it is not restricted to the determination of the epoch state vector but also allows the estimation of the full set of force model parameters in the bundle adjustment.

While radio tracking is related to the spacecraft's inertial position, the images of known surface features on ground establish the position in a body-fixed reference frame. By combining both data types, the transformation between the body-fixed and the inertial reference frame, represented by the planetary rotation parameters, may be improved within the bundle adjustment procedure.

2.2 New Approach

The photogrammetric evaluation of 3-line imagery starts with the precise reconstruction of the exterior orientation of the images and the determination of ground points within the scope of a bundle block adjustment. The mathematical model of bundle block adjustment is based on the collinearity equations

$$u = u(x, x^c(t), \theta(t)) \quad , \tag{1}$$

which formulate the relationship between the observed image coordinates $u = (u_x, u_y)^T$, the unknown object point coordinates $x = (X, Y, Z)^T$ of a point P and the unknown parameters of exterior orientation $x^c = (X^c, Y^c, Z^c)^T$ and $\theta = (\zeta, \eta, \theta)^T$, respectively, of the image I_j. The orientation angles ζ, η and θ have to be chosen in such a way that singularities are avoided. In space photogrammetry the three Euler angles, which are related to the spacecraft motion along the trajectory, are well suited in conjunction with a geocentric object coordinate system.

Due to the dynamical mode of image acquisition, each image line I_j has its own exterior orientation with 6 unknown orientation parameters. Since the existing image and control information is not sufficient to estimate all unknowns, the 6 orientation parameters are treated as unknowns only for so-called orientation points, which are introduced at certain time intervals, e.g. once for every 100th or 1000th readout cycle. In between, the orientation parameters of each image line are expressed as polynomials of the parameters of the neighbouring orientation points (Ebner et al. 1994a).

While this approach reduces the number of unknown orientation parameters to a reasonable amount, it has several disadvantages:

- Any physical relation between the exterior orientation at subsequent orientation points is neglected entirely, since the positions are modeled by piecewise polynomials and not by orbital constraints.

- The statistical properties of the position data de-

rived from orbit determination are improperly considered in the bundle adjustment.

- The positional exterior orientation parameters estimated in the bundle adjustment do not permit an interpretation in terms of physical parameters.

In order to avoid these disadvantages, a new approach has been developed, which guarantees that all exposure stations of the cameras are lying on a physically consistent trajectory. To this end, the position parameters x^c, which have been estimated so far at arbitrary orientation points, are now replaced by the 6 parameters of the epoch state vector y_0 and additional force model parameters p. The force model parameters p may comprise e.g. the drag coefficient C_D and the solar radiation pressure coefficient C_R. In addition, epoch state vector and force model parameters are introduced into the bundle adjustment as direct observations with their full covariance information. Statistically, the resulting estimation procedure is equivalent to a combined orbit determination and bundle adjustment from radio tracking data and 3-line image data.

Fig. 1 demonstrates the fundamental difference between the conventional and the combined model. In the conventional model (left), the position parameters are assumed as independent of the flight behaviour of the spacecraft, which may result in an unrealistic trajectory. However, the combined model (right) exploits the fact that the spacecraft proceeds along an orbit trajectory and all scanner positions lie on this trajectory, when estimating the spacecraft's epoch state vector.

The combined model has essential advantages for the point determination task, which can be summarized as follows:

- Full utilization of the information contents of the tracking data in a statistically consistent way.

- A reduced number of unknown exterior orientation parameters, which stabilizes the solution of the normal equations.

- The results of the combined bundle adjustment allow a scientific interpretation of the camera position, as they satisfy the physical laws of motion on a satellite trajectory.

Thus tracking data and 3-line imagery will contribute to the estimation of photogrammetric as well as orbit parameters.

Due to the lack of a dynamical model describing the camera's attitude behaviour during an imaging sequence, it is not possible to introduce attitude constraints into the bundle adjustment in a similar way as the orbital constraints. To this end, the concept of orientation points is maintained for the spacecraft's attitude.

2.3 Mathematical Model

To include orbital constraints, the camera position and hence the image coordinates have to be expressed as a function of the satellite's epoch state vector y_0 and the force model parameter vector p:

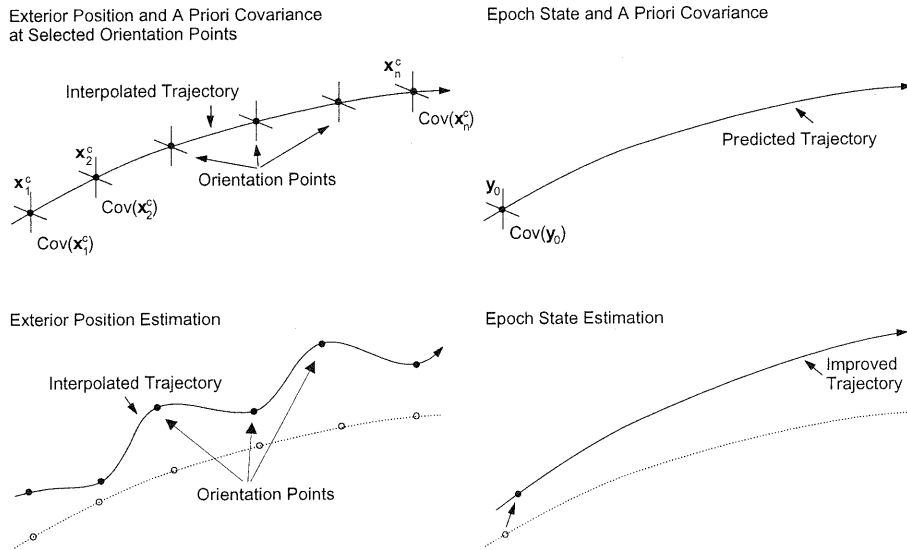$$x^c(t) = x^c(t, y_0, p) \tag{2}$$

598

Figure 1: Airborne (left) and spaceborne (right) model for the reconstruction of the exterior orientation of 3-line images (Montenbruck et al. 1994)

The attitude

$$\boldsymbol{\theta}(t) = \boldsymbol{\theta}(t, \boldsymbol{\Theta}, \beta) \qquad (3)$$

of the camera can be represented by the attitude vector $\boldsymbol{\Theta}$ at selected orientation points and a vector β including additional bias and drift parameters. Based on (2) and (3), the image coordinates may be written as

$$\boldsymbol{u} = \boldsymbol{u}(\boldsymbol{x}, \boldsymbol{x}^c(t), \boldsymbol{\theta}(t)) = \boldsymbol{u}(t, \boldsymbol{x}, \boldsymbol{y}_0, \boldsymbol{p}, \boldsymbol{\Theta}, \beta) \quad , \quad (4)$$

while the partial derivatives required in the adjustment are given by

$$\frac{\partial \boldsymbol{u}}{\partial \boldsymbol{y}_0} = \frac{\partial \boldsymbol{u}}{\partial \boldsymbol{x}^c} \frac{\partial \boldsymbol{x}^c}{\partial \boldsymbol{y}_0} \quad , \qquad (5)$$

$$\frac{\partial \boldsymbol{u}}{\partial \boldsymbol{p}} = \frac{\partial \boldsymbol{u}}{\partial \boldsymbol{x}^c} \frac{\partial \boldsymbol{x}^c}{\partial \boldsymbol{p}} \quad \text{and} \qquad (6)$$

$$\frac{\partial \boldsymbol{u}}{\partial \boldsymbol{\Theta}} = \frac{\partial \boldsymbol{u}}{\partial \boldsymbol{\theta}} \frac{\partial \boldsymbol{\theta}}{\partial \boldsymbol{\Theta}} \quad . \qquad (7)$$

Here the partials of $\boldsymbol{x}^c$ with respect to $\boldsymbol{y}_0$ and $\boldsymbol{p}$ are obtained from the variational equations which are solved simultaneously with the equation of motion. The required partial derivatives (7) are achieved by differentiation of the collinearity equations and the polynomial interpolation formula. The mathematical model of the combined bundle adjustment approach is described in detail in Montenbruck et al. (1994) and Ohlhof (1995).

3 COMPUTER SIMULATIONS ON LOCAL, REGIONAL AND GLOBAL POINT DETERMINATION

3.1 Mars96 HRSC/WAOSS Experiment

The High Resolution Stereo Camera (HRSC) and the Wide-Angle Optoelectronic Stereo Scanner (WAOSS) were designed to be flown towards planet Mars on board a Russian spacecraft in November 1996. The orbit of the Mars96

spacecraft will be elliptic with a periapsis height of 300 km and an apoapsis height of 22 000 km.

HRSC is a one-lens camera and contains 3 identical sensor plates in the focal plane which can be called according to the geometric arrangement the forward, the nadir and the backward (looking) plate, respectively. Each plate consists again of 3 CCD sensor arrays (Thompson THX 7808) and each array of 5184 active elements. In the nadir plate the middle (nadir looking) CCD array is a panchromatic channel, the other 2 arrays are green and blue channels. In the forward plate the outermost CCD array represents a panchromatic stereo channel, the innermost array another panchromatic channel for photometric purposes and the middle array an infrared channel. The same is in the backward plate except that the infrared channel is replaced by a purple one. The ground pixel size at periapsis is 12 m for all channels if no formation of macropixels takes place. The photogrammetric processing is mainly based on imagery of the nadir and the two stereo channels.

Like HRSC, WAOSS is a one-lens camera but consists of one sensor plate in the focal plane only. The plate of WAOSS is identical to those used in the HRSC. All 3 CCD arrays are panchromatic channels and will have a ground pixel size of 97 m at periapsis. As there is no separate color capability with WAOSS, slightly different filters will be used.

Besides image information represented by a large amount of conjugate points which are measured automatically, control information is required for point determination. Due to the lack of accurate ground control points and navigation systems like GPS or INS, orbit and attitude determination of the Mars96 spacecraft are of high importance. The orbit determination is based on range and Doppler tracking between the Mars96 spacecraft and ground stations on Earth, and attitude information is derived from gyro readings and images taken by a star camera. A detailed description of the HRSC experiment and the photogrammetric processing chain is given by Albertz et al. (1993) and Ebner et al. (1994b).

599

International Archives of Photogrammetry and Remote Sensing. Vol. XXXI, Part B3. Vienna 1996

	Local PD	Regional PD	Global PD
Images	HRSC	HRSC, WAOSS	WAOSS
Datum definition	local	local or global	global
Block configuration	single strips; small blocks of overlapping or crossing strips	large blocks of many overlapping strips	closed block covering the entire surface
Computation effort	moderate	high	very high
Accuracy local	very high	high	high
Accuracy global	low	moderate	high

Table 1: Local, regional and global point determination (PD) on Mars and their characteristics

3.2 Local, Regional and Global Point Determination

The point determination (PD) on Mars will be carried out at local, regional and global levels (Table 1).

HRSC will mainly operate in the near periapsis region, so that about 10–20% of the Martian surface can be imaged by HRSC with a ground pixel size of 12–20 m. The local PD is therefore based on HRSC images and implies the simultaneous adjustment of several crossing or overlapping strips, which will be aquired around the periapsis with a nearly constant ground pixel size.

The regional PD comprises the adjustment of large blocks of many overlapping strips and is based on a combined evaluation of HRSC and WAOSS images.

Image sequences for WAOSS are planned for orbital positions up to 90° true anomaly. Thus WAOSS images will cover the entire planet with 100–1000 m ground pixel size, so that a closed block triangulation with complete overlap in all three directions may be carried out.

3.3 Computer Simulations

Comprehensive computer simulations on local, regional and global PD have been performed to obtain a survey of the attainable local and global accuracies and to give recommendations in the planning phase of the Mars96 mission. The results of these simulations are summarized in Table 2.

The local accuracy represents the interior accuracy of PD, as the influence of the datum definition is excluded using the method of free adjustment. The global accuracy, in contrast, stands for the exterior accuracy of PD referring to the Mars-fixed reference system.

	Local Accuracy $\mu_{\hat{X}\hat{Y}}$[m]	Local Accuracy $\mu_{\hat{Z}}$[m]	Global Accuracy $\mu_{\hat{X}\hat{Y}}$[m]	Global Accuracy $\mu_{\hat{Z}}$[m]
Local PD	5	10	300	50
Regional PD	15	30	100	30
Global PD	40	40	60	60

Table 2: Attainable planimetric and height accuracies (1σ) of adjusted object point coordinates for the local, regional and global PD on Mars

The local PD mainly depends on the number, distribution and precision of conjugate points and benefits from the high relative accuracy of the orbit and attitude data. The local accuracy can be considerably improved to about 5 m in planimetry and 10 m in height, if the 2 photometric channels of HRSC are incorporated into the bundle adjustment (Fig. 2).
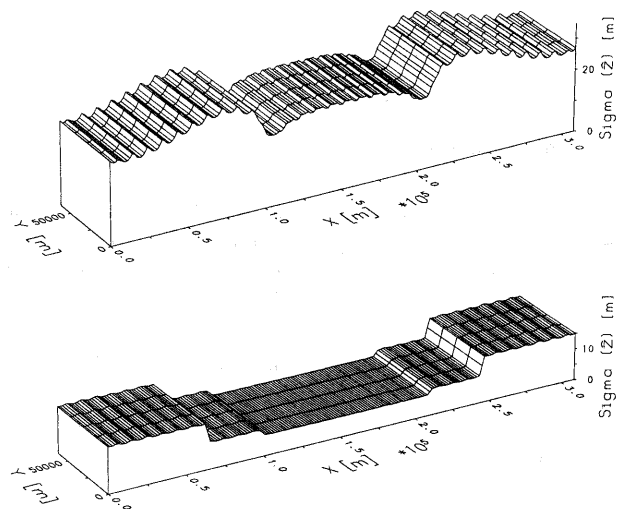

Figure 2: Standard deviations of adjusted $\hat{Z}$ coordinates of the object points for HRSC with 3 CCD arrays (above) and with 5 CCD arrays (below)

A large number of simulation runs on regional PD have shown that most accurate results can be achieved by combining HRSC and WAOSS data and by the simultaneous block adjustment of multiple overlapping strips with $\geq$60% side lap and additional crossing strips at the borders of the block (Ebner et al. 1994b, Ohlhof 1995).

Since WAOSS will image the entire planet, a global block with complete overlap in all directions may be processed under ideal circumstances. Because of the extraordinary strength of the closed block and based on the complete image, orbit, attitude and ground control information, 60 m global accuracy in planimetry and height can be achieved.

In summary, it can be stated that the synergy effect of image and orbit information is most effective, if many overlapping orbital arcs are processed simultaneously in a block with high geometric strength. It can be expected that the accuracy of the current ground control network of Mars is generally improved by a factor of 10 or more.

600

International Archives of Photogrammetry and Remote Sensing. Vol. XXXI, Part B3. Vienna 1996

3.4 Mars rotation parameters

In case of the global PD, special emphasize is given to the Mars rotation parameters, which define the link between the Mars-fixed object coordinate system as the reference frame for photogrammetry, and the inertial Earth equator and equinox of J2000 coordinate system as the reference frame for orbit determination. By combining image and radio tracking data, as described in section 2, the Mars rotation parameters may be treated as estimation parameters within the bundle adjustment.

The Mars-fixed system is aligned with the Mars equator where the prime meridian is defined by the small crater Airy-0. The orientation of the Mars equator and the so-called IAU vector is described by the right ascension α and declination δ of the Mars north pole with respect to the Earth mean equator and equinox of J2000. Here, the IAU vector is defined as the intersection line of the planes described by the Earth equator of J2000 and the Mars equator (Davies et al. 1992). The rotation of planet Mars is described by the parameter W giving the angle between the IAU vector and the point where the prime meridian through the crater Airy-0 intersects the Martian equator. Therefore, three elementary rotations are required for the transformation from J2000 coordinates to the Mars-fixed equator and prime meridian coordinates (Fig. 3):

1st rotation around the z-axis by an angle $(90° + \alpha)$ that is equal to the right ascension of the IAU vector,

2nd rotation around the x'-axis by an angle $(90° - \delta)$ that is equal to the angle between the Mars equator and the Earth equator

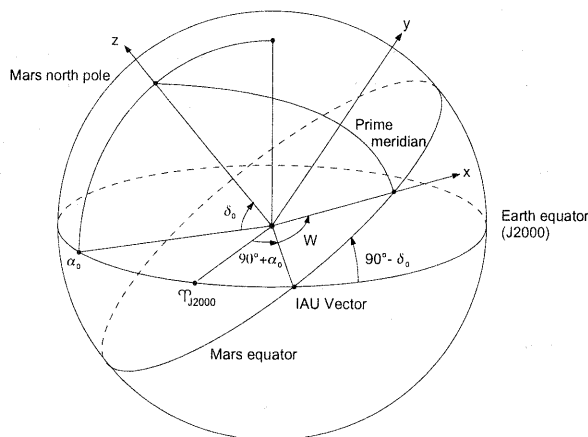3rd rotation around the z''-axis by an angle $(-W)$.

Figure 3: Orientation of the north pole and prime meridian of Mars with respect to the Earth equator and equinox of J2000

Neglecting nutation, the right ascension α, declination δ, and W are generally expressed as linear polynomials

$$\alpha(t) = \alpha_0 + \dot{\alpha} T$$
$$\delta(t) = \delta_0 + \dot{\delta} T \qquad (8)$$
$$W(t) = W_0 + \dot{W} d$$

in time, where the subscript $_0$ refers to the orientation of the Mars rotation axis at the reference epoch J2000 and T is the ephemeris time in Julian centuries since that epoch. The parameters W_0 and $\dot{W}$ denote the longitude of the prime meridian with respect to the IAU vector at J2000 and the rotation rate, while d gives the ephemeris time in days elapsed since that epoch. Note that $\dot{\alpha}$ and $\dot{\delta}$ arise from precession and might be expressed as functions of the Mars precession rate $\langle \dot{\psi} \rangle$. The parameters that affect the transformation from the inertial to the body-fixed system may therefore be combined to a planetary rotation parameter vector $\boldsymbol{\omega} = (\alpha_0, \delta_0, \langle \dot{\psi} \rangle, W_0, \dot{W})^T$.

It can be seen from Fig. 4 that the accuracies of the Mars rotation parameters in the global block adjustment can be improved up to factor 4. Further information on this topic is given by Ohlhof (1995).
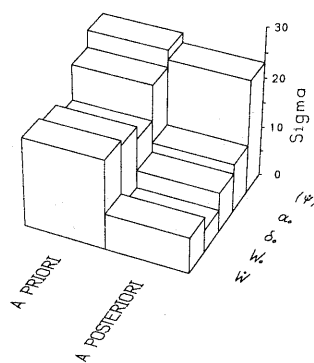

Figure 4: Standard deviations a priori und a posteriori of the Mars rotation parameters ($\langle \dot{\psi} \rangle[''/\text{cy}]$, $\alpha_0['']$, $\delta_0['']$, $W_0[°\cdot 1000]$, $\dot{W}[''/\text{d} \cdot 1000]$) for the global Mars block

4   PRACTICAL TEST USING MOMS-02/D2 DATA

4.1   MOMS-02/D2 Experiment

During the 2nd German spacelab mission D2, successfully flown in April/May 1993, the Modular Optoelectronic Multispectral Stereo Scanner MOMS-02 acquired digital high resolution, multispectral and 3-fold stereoscopic imagery of the earth surface.

The optical system of MOMS-02 consists of a stereo module and a multispectral module. The 3 lenses of the stereo module with 1 CCD sensor array.(Fairchild 191) each provide 3-fold along track stereo scanning with different ground resolutions. The nadir looking CCD array (4.5 m ground pixel size) comprises 2 arrays with 6000 sensor elements each, which are optically combined to 1 array with 9000 active sensor elements. The other CCD arrays of the stereo module consist of 6000 active sensor elements (13.5 m ground pixel size).

To verify the concept of orbital constraints in the photogrammetric restitution of MOMS-02 imagery, one imaging sequence with 3 image strips and 32 120 rows each covering 430 × 37 km² in North-West Australia (orbit #75B) has been selected.

4.2 Preprocessing

The photogrammetric restitution of 3-line imagery requires a large number of conjugate points. Digital image matching is an appropriate technique to automatically determine these points. Before starting the matching procedure, the image strip of the nadir looking CCD array was resampled by factor 3 to obtain the same pixel size in all 3 strips. Using the least squares *region-growing* matching algorithm (Heipke et al. 1994) about 14 000 conjugate points were found. The standard deviation of the image coordinates was assumed to be 0.3 pixel.

In the area covered by the 3 image strips 79 DGPS-derived ground control points (GCP) were available with a standard deviation of 0.1 m in X, Y and Z. 75 points were identified and measured in the images (Baltsavias 1995).

During the D2 mission tracking was routinely performed using the Tracking and Data Relay Satellite System (TDRSS). The orbit determination for orbit #75B is based on 900 S-Band Doppler measurements with a sampling rate of 10 s covering about 180 minutes. The force and measurement modeling comprises the shuttle epoch state vector, the drag coefficient and 5 parameters describing perturbations of the attitude thruster system. The pure statistical standard deviations of the epoch state vector components were 30 m, whereas unmodeled effects of the attitude thruster system contribute an additional error of up to 50 m (Braun, Reigber 1994).

A major problem arose from the fact that the image recording times could in general not be related better than 0.5 s to the time scale UTC. A time offset of 0.5 s corresponds to an along-track position offset of the space shuttle of $0.5 \, \text{s} \cdot 7 \, \text{km/s} = 3.5 \, \text{km}$ (!). Since no parameter for the time offset exists in the bundle adjustment algorithm, a realistic weighting matrix for the epoch state vector components has been derived to relax the orbital constraints in the along-track direction (Gill et al. 1995). The force model parameters p were treated as constants due to the short time span (1 min) of image acquisition.

Attitude information was derived from gyro recordings of the Inertial Measurement Units (IMU) of the shuttle Guidance Navigation and Control System. Based on approximation tests the optimum distance between two orientation points was found to be 4615 rows, corresponding to a flight distance of 62.3 km and a flight time of 9.1 s.

4.3 Combined Bundle Adjustment

The combined bundle adjustment was performed in the geocentric coordinate system WGS84. The DGPS-derived ground points were divided into two groups. The first group consists of 12 GCP, where 3 points each are located in the corners of the threefold overlapping area to ensure a precise definition of the global datum. The second group comprises 63 geometrically well distributed points which were used as check points.

The following data were introduced as observations:

- Image coordinates of 13 959 conjugate points ($\sigma = 0.3$ pixel)
- Image coordinates of 12 GCP ($\sigma = 0.5$ pixel)
- Image coordinates of 63 check points ($\sigma = 0.5$ pixel)

- Object coordinates of 12 GCP ($\sigma_X = \sigma_Y = \sigma_Z = 0.1$ m)
- Epoch state vector components with associated 6×6 weighting matrix
- Attitude parameters (ζ, η, θ) at 8 orientation points ($\sigma_\zeta = \sigma_\eta = \sigma_\theta = 50''$)

In Table 3 the rms values of the theoretical standard deviations of the check point coordinates $\hat{X}$, $\hat{Y}$ and $\hat{Z}$ and the corresponding empirical values are presented. The theoretical values were computed from the inverted normal equation matrix and the a posteriori $\hat{\sigma}_0$ value of the bundle adjustment. The empirical values were derived by comparing the estimated object coordinates of the check points and the known values.

MOMS #75B		theor.	empir.
$\mu_{\hat{X}}$	[m]	11.2	9.3
$\mu_{\hat{Y}}$	[m]	13.1	10.2
$\mu_{\hat{Z}}$	[m]	8.9	11.2
$\mu_{\hat{X}\hat{Y}\hat{Z}}$	[m]	11.2	10.3

Table 3: Rms values $\mu_{\hat{X}}$, $\mu_{\hat{Y}}$, $\mu_{\hat{Z}}$ and $\mu_{\hat{X}\hat{Y}\hat{Z}}$ of the theoretical standard deviations derived from 63 check points and corresponding empirical values

The good correspondence between the theoretical and the empirical values proves the correctness of the stochastic and the functional model. The empirical values show that accuracies of about 10 m (0.7 pixel) in X, Y and Z were achieved. A graphical analysis of the residuals in the check points showed that the results are not affected by systematic errors.

Due to the improper time synchronization between image and orbit data, large corrections to the a priori state vector components occured, that contribute mainly to along-track position errors. The theoretical accuracy of the six components was improved compared to the a priori values by a factor of 6 to a level of 150 m, primarily due to the availability of GCP. The orbit accuracy from the pure TDRSS solution (50–70 m), however, could not be improved. A high accuracy orbit determination from a combined bundle adjustment thus requires a time synchronization of 0.1 ms or better.

5 CONCLUSIONS AND OUTLOOK

In this paper a new concept for integrated orbit and point determination in satellite photogrammetry is presented and verified by simulated Mars96 HRSC/WAOSS and practical MOMS-02/D2 data. For the first time orbit determination results are rigorously incorporated into the bundle block adjustment, which is equivalent to a combined adjustment of tracking and image data. The proposed concept guarantees the proper utilization of orbit information in the bundle adjustment and, vice-versa, enables the use of image information to improve the orbit determination and to support the estimation of scientific parameters (e.g. Mars rotation parameters).

602

International Archives of Photogrammetry and Remote Sensing. Vol. XXXI, Part B3. Vienna 1996

The new concept will be routinely used for the forthcoming MOMS-2P/PRIRODA mission aboard the Russian space station MIR, scheduled for spring 1996. Within 18 months MOMS-2P (MOMS-02, adapted to the PRIRODA environment) will collect imagery from about 400 km orbital height with a ground resolution of 6 m and 18 m respectively. The dedicated MOMSNAV navigation package, consisting of high precision GPS and INS ensures precise orbit and attitude data, synchronized with the MOMS-2P imagery by 0.1 msec. Since MOMS-2P/PRIRODA images will enable a regional covering, a simultaneous block adjustment of several overlapping strips from different orbit arcs which provides highly accurate results will be possible.

Another attractive application of the integrated concept is based on 79 images of Ida and its satellite Dactyl obtained by a CCD frame camera during the 2nd Galileo asteroid flyby in August 1993. These images combined with orbit and attitude data and orbital constraints provide a novel opportunity to extract the physical parameters of Ida and Dactyl, i.e. size, shape and motion of the two objects, as well as possibly also mass and density of Ida.

6 ACKNOWLEDGEMENTS

7 REFERENCES

Albertz J., Scholten F., Ebner H., Heipke C., Neukum G. (1993): Two Camera Experiments on the Mars94/96 Missions; GIS 6(4), 11–16.

Baltsavias E. (1995): Private Communication.

Braun C.v., Reigber C. (1994): Space shuttle orbit determination using empirical force modelling of attitude maneuvers for the German MOMS-02/D2 mission; Flight Mechanics and Estimation Theory Symposium, Goddard Space Flight Center, May 17-19, Greenbelt.

Case J.B. (1961): The Utilization of Constraints in Analytical Photogrammetry; Photogrammetric Engineering 25(5), 766–788.

Davies M.E., Abalakin V.K., Brahic A., Bursa M., Chovitz B.H., Lieske J.H., Seidelmann P.K., Sinclair A.T., Tjuflin Y.S. (1992): Report of the IAU/IAG/COSPAR Working Group on Cartographic Coordinates and Rotational Elements of the Planets and Satellites: 1991; Celestial Mechanics 53, 377–397.

Davis R., Riding T. (1970): The Rigorous and Simultaneous Adjustment of Lunar Orbiter Photography Considering Orbital Constraints; RADC-TR-70-274, Rome Air Development Center, National Technical Information Center, Springfield, Virginia.

Ebner H., Kornus W., Ohlhof T. (1994a): A simulation study on point determination for the MOMS-02/D2 Space Project using an extended functional model; GIS 7(1), 11–16.

Ebner H., Ohlhof T, Tang L. (1994b): Eine Studie zur Bildzuordnung und Punktbestimmung im Rahmen der Mars94-Mission; Zeitschrift für Photogrammetrie und Fernerkundung 62(2), 57–71.

Eckardt A. (1995): The performance of the new Wide Angle Airborne Camera (WAAC); Int. Arch. of Photogrammetry and Remote Sensing 30(5W1), 26–29.

Gill E., Montenbruck O., Ohlhof T., Schmidhuber M. (1995): First results on shuttle orbit adjustment using MOMS-02 imagery; Proc. of the Int. Space Dynamics Symp., June 19-23, Toulouse, 917–929.

Heipke C., Kornus W., Pfannenstein A. (1994): The evaluation of MEOSS airborne 3-line scanner imagery – processing chain and results. Int. Arch. of Photogrammetry and Remote Sensing 30(4), 239–250.

Lanzl F. (1986): The Monocular Electro-Optical Stereo Scanner (MEOSS) satellite experiment; Int. Arch. of Photogrammetry and Remote Sensing, 26(1), 617–620.

Lehner M., Drescher A. (1987): MEOSS, Modelling of short orbit arcs using Brouwer mean elements or polynomials (least squares approximation tests); DFVLR Internal Report, Oberpfaffenhofen.

Light D.L. (ed) (1980): Satellite Photogrammetry; in: Manual of Photogrammetry, American Society of Photogrammetry, 4th edition, 883–977.

Masaharu H. (1989): Modelling of Short Arc Orbital Constraints for Incorporation into Photogrammetric Adjustment of MEOSS Data; DFVLR-FB 89-14, Oberpfaffenhofen.

Montenbruck O., Gill E., Ohlhof T. (1994): A Combined Approach for Mars-94 Orbit Determination and Photogrammetric Bundle Adjustment; DLR-Forschungsbericht 94-13, 95 p.

Müller F., Hofmann O., Kaltenecker A. (1994): Digital Photogrammetric Assembly (DPS) point determination using airborne three-line camera imagery: practical results. Int. Arch. of Photogrammetry and Remote Sensing 30(3/2), 592–598.

Murai S., Matsumoto Y., Li X. (1995): Stereoscopic imagery with an airborne 3-line scanner (TLS); Int. Arch. of Photogrammetry and Remote Sensing 30(5W1), 20–25.

Neukum G., Oberst J., Schwarz G., Flohrer J., Sebastian I., Jaumann R., Hoffmann H., Carsenty U., Eichentopf K., Pischel R. (1995): The Multiple Line Scanner Camera Experiment for the Russian Mars96 Mission: Status Report and Prospects for the Future; in: Photogrammetric Week '95, edited by D. Fritsch and D. Hobbie, Wichmann, Karlsruhe, 45–61.

Ohlhof T. (1995): Lokale, regionale und globale Punktbestimmung mit Bild- und Bahninformation der Mars96-Mission; PhD thesis, Deutsche Geodätische Kommission, C 445, 139 p.

Sandau R., Bärwald W. (1994): A three-line wide-angle CCD stereo camera for Mars-94 mission; Int. Arch. of Photogrammetry and Remote Sensing 30(1), 82–86.

Seige P. and D. Meissner D. (1993): MOMS-02: An advanced high resolution multispectral stereo scanner for Earth observation; GIS 6(1), 4–11.

Westin T. (1990): Precision Rectification of SPOT Imagery; Photogrammetric Engineering and Remote Sensing 56(2), 247–253.

603

International Archives of Photogrammetry and Remote Sensing. Vol. XXXI, Part B3. Vienna 1996